Journal of Power Sources 195 (2010) 5596–5600

Contents lists available at ScienceDirect

Journal of Power Sources

journal homepage: www.elsevier.com/locate/jpowsour

Short communications

Intermediate temperature ionic conduction in $Sn_{1-x}Ga_xP_2O_7$

Hongtao Wang[a,b], Jinwei Liu[a], Wenbao Wang[a], Guilin Ma[a,*]

[a] Key Laboratory of Organic Synthesis of Jiangsu Province, College of Chemistry, Chemical Engineering and Materials Science, Soochow University, Suzhou 215123, China
[b] College of Chemistry and Chemical Engineering, Fuyang Teachers College, Fuyang 236041, China

ARTICLE INFO

Article history:
Received 11 January 2010
Received in revised form 29 March 2010
Accepted 29 March 2010
Available online 2 April 2010

Keywords:
Tin pyrophosphate
Ionic conduction
Gas concentration cell
Isotope effect
Fuel cell

ABSTRACT

A novel series of samples $Sn_{1-x}Ga_xP_2O_7$ ($x = 0.00, 0.01, 0.03, 0.06, 0.09, 0.12, 0.15$) are synthesized by solid state reaction. XRD patterns indicate that the samples of $x = 0.00 - 0.09$ exhibit a single cubic phase structure, and the doping limit of Ga^{3+} in $Sn_{1-x}Ga_xP_2O_7$ is $x = 0.09$. The protonic and oxide-ionic conduction in $Sn_{1-x}Ga_xP_2O_7$ are investigated using some electrochemical methods at intermediate temperatures (323–523 K). It is found that the samples exhibit appreciable protonic conduction in hydrogen atmosphere, and a mixed conduction of oxide-ion and electron hole in dry oxygen-containing atmosphere. The highest conductivities are observed for the sample of $x = 0.09$ to be 4.6×10^{-2} S cm^{-1} in wet H_2 and 2.9×10^{-2} S cm^{-1} in dry air at 448 K, respectively. The H_2/air fuel cell using $x = 0.09$ as electrolyte (thickness: 1.45 mm) generates a maximum power density of 19.2 mW cm^{-2} at 423 K and 22.1 mW cm^{-2} at 448 K, respectively.

1. Introduction

Fuel cells have been attracted increasing attention because they cleanly and high efficiently convert chemical energy directly to electrical energy, etc. [1–6]. As well known, high temperature fuel cells (HTFCs) using doped $BaCeO_3$, $LaGaO_3$ and YSZ etc. as electrolytes display high output powers at 773–1273 K [7–9]. However, for practical applications, the sealing and bonding materials of HTFCs are required to have high and sustainable stability at elevated temperatures. Proton exchange membrane fuel cells (PEMFCs) using proton-conducting perfluorinated polymer Nafion as solid electrolyte can attain high power densities and efficiencies at temperatures below 373 K. However, PEMFCs based on Nafion have some disadvantages, such as sluggish kinetics of both anode and cathode reactions, water permeability through the polymer electrolyte membrane, CO poisoning of the platinum catalyst and very limited lifetime etc. at low operating temperatures [10–12]. Considerable effort has been devoted toward the intermediate temperature fuel cells (ITFCs) based on $CsHSO_4$, CsH_2PO_4 etc. in the temperature range of 423 to 673 K [5,13]. Recently, a new type intermediate temperature protonic conductor, $Sn_{1-x}R_xP_2O_7$ ($R = Al^{3+}$, In^{3+}, Sb^{3+}, Mg^{2+}), is attracted considerable attention for their potential applications in ITFCs, gas sensors and electrochemical reactors etc. [14–23]. Hibino et al. reported that the H_2/air fuel cell using $Sn_{0.9}In_{0.1}P_2O_7$ as an electrolyte (thickness: 0.35 mm) yields a power density of 264 mW cm^{-2} under unhumidified conditions at 523 K [23]. Wang et al. reported that the fuel cell using $Sn_{0.9}In_{0.1}P_2O_7$ as an electrolyte (thickness: 0.78 mm) yields power densities of 14.9 mW cm^{-2} under $H_2 + CH_3OH/O_2$ and 14.7 mW cm^{-2} under H_2/O_2 conditions at 443 K, respectively [17]. Hibino et al. also applied proton-conducting $Sn_{1-x}R_xP_2O_7$ ($R = In^{3+}$, Al^{3+}) to some electrochemical reactors, such as a selective catalytic reduction of NO_x to form N_2 and H_2O, a direct oxidation of methane to methanol, and gas sensors, etc. [15,19–22].

Ga^{3+} is not only the same main group element as Al^{3+} and In^{3+}, but also the effective ionic radius (0.062 nm [24]) of Ga^{3+} is close to that (0.069 nm [24]) of Sn^{4+} in 6-fold coordination. Therefore, it is interesting to investigate the $Sn_{1-x}Ga_xP_2O_7$. In this study, a novel series of intermediate temperature solid ion conductors, $Sn_{1-x}Ga_xP_2O_7$ ($x = 0.00, 0.01, 0.03, 0.06, 0.09, 0.12, 0.15$), was prepared and the proton and oxide-ion conduction was investigated using some electrochemical methods at intermediate temperatures (323–523 K). A hydrogen-air fuel cell using $Sn_{0.91}Ga_{0.09}P_2O_7$ with the highest conductivity as an electrolyte was constructed and the feasibility applying this material to intermediate temperature fuel cells was also explored.

2. Experimental

2.1. Preparation and characterization of $Sn_{1-x}Ga_xP_2O_7$

$Sn_{1-x}Ga_xP_2O_7$ ($x = 0.00, 0.01, 0.03, 0.06, 0.09, 0.12, 0.15$) was prepared as follows. The required amounts of SnO_2 (Luoyang Ship Material Research Institute, 50–70 nm), Ga_2O_3 (99.9%) and 85% H_3PO_4 were fully mixed and held with stirring around 623 K until they became solid mixtures. Then the solid mixtures were heat-

* Corresponding author. Tel.: +86 512 65880326; fax: +86 512 65880089.
E-mail address: 32uumagl@suda.edu.cn (G. Ma).

0378-7753/$ – see front matter © 2010 Elsevier B.V. All rights reserved.
doi:10.1016/j.jpowsour.2010.03.087

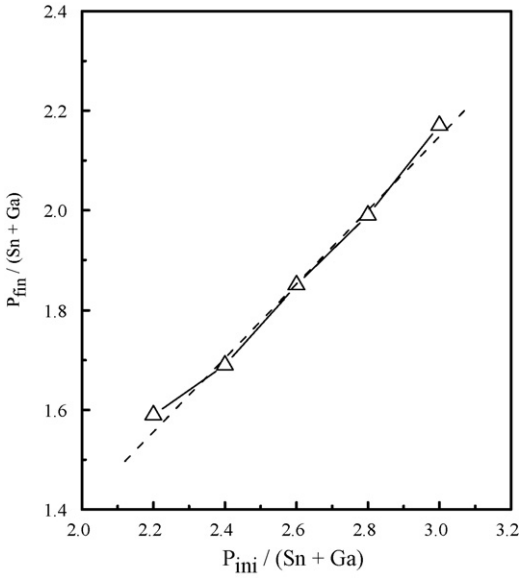

Fig. 1. The final $P_{fin}/(Sn+Ga)$ molar ratios as a function of the initial $P_{ini}/(Sn+Ga)$ molar ratios for $x = 0.06$ sample.

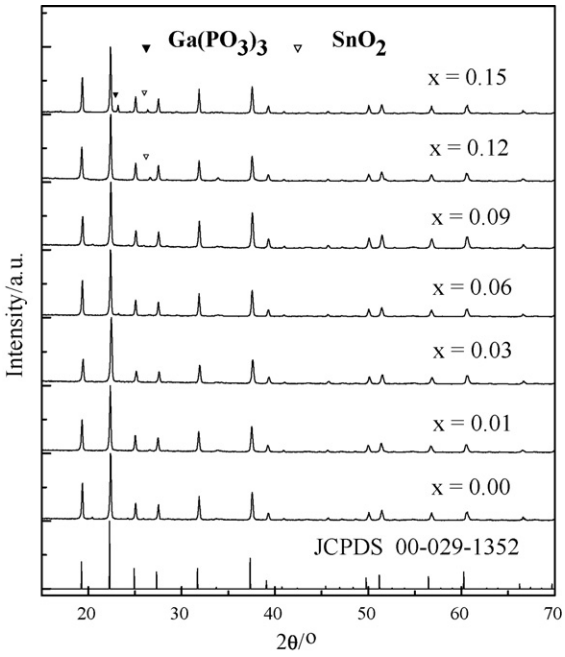

Fig. 2. XRD patterns of the $Sn_{1-x}Ga_xP_2O_7$ ($x = 0.00 - 0.15$) samples.

treated at 873 K for 2 h to obtain $Sn_{1-x}Ga_xP_2O_7$ powders. The final molar ratios of phosphorus vs. metal ions, $P_{fin}/(Sn+Ga)$, in the powders were evaluated through X-ray fluorescence (XRF) measurement. The crystalline structure of the $Sn_{1-x}Ga_xP_2O_7$ powders was determined at room temperature by X-ray diffraction (XRD) analysis.

2.2. Electrochemical measurements

The powders were pressed into pellets (diameter 20 mm, thickness 1.4–2.2 mm) at a hydrostatic pressure of 300 MPa. Platinum paste was coated on both sides (area: 0.5 cm^2) of the pellets and heated at 523 K for 30 min. The pellets were connected to Pt wires and sealed between two alumina tubes, and then placed into an electric furnace for electrochemical measurements. To estimate the contribution of ions to the conduction, the electromotive forces of oxygen and hydrogen concentration cells with $Sn_{1-x}Ga_xP_2O_7$ pellets as the electrolytes were measured. The isotope effect on conductivity was applied to examine the proton conduction in water vapor-containing atmosphere. The conductivity measurements were carried out by an AC impedance method using electrochemical workstations (Zahner IM6ex) over the frequency range from 1 Hz to 3 MHz in dry air and wet H_2 atmospheres at 323–523 K. For the experimental atmospheres, wet gases were obtained by saturating water vapor at 298 K and dry gases were obtained by using a cold trap based on low temperature nitrogen gas (ca. 153 K). The H_2/air fuel cell using $Sn_{0.91}Ga_{0.09}P_2O_7$ as an electrolyte and porous platinum as cathode and anode was constructed. The current–voltage curves were measured to evaluate the performance of the fuel cell.

3. Results and discussion

3.1. Effect of Ga^{3+} doping level on phase purity

Due to a fraction of phosphorus loss in the process by vaporization [15,18], the final molar ratios of phosphorus vs. metal ions, $P_{fin}/(Sn+Ga)$, as a function of the initial molar ratios of phosphorus vs. metal ions, $P_{ini}/(Sn+Ga)$, are investigated. Fig. 1 shows a representative relationship of $P_{fin}/(Sn+Ga) \sim P_{ini}/(Sn+Ga)$ for $x = 0.06$ sample. It is found that the corresponding $P_{fin}/(Sn+Ga)$ increases with increasing $P_{ini}/(Sn+Ga)$ from 2.2 to 3.0, and reaches 2.0 when $P_{ini}/(Sn+Ga)$ is 2.8. Therefore, $P_{ini}/(Sn+Ga)$ should be controlled to be 2.8.

Fig. 2 shows XRD patterns at room temperature of the $Sn_{1-x}Ga_xP_2O_7$ samples. As shown, $Sn_{1-x}Ga_xP_2O_7$ ($x = 0.00 - 0.09$) is in agreement with the cubic phase structure of SnP_2O_7 in JCPDS (00-029-1352). Besides, $Sn_{1-x}Ga_xP_2O_7$ ($x = 0.12$) has some additional peaks of SnO_2 impurity, and $Sn_{1-x}Ga_xP_2O_7$ ($x = 0.15$) has some additional peaks of $Ga(PO_3)_3$ and SnO_2 impurities, indicating the doping limit of Ga^{3+} in SnP_2O_7 is 9 mol%.

3.2. Effect of Ga^{3+} doping level on electrochemical properties

To investigate the oxide-ion conduction in dry oxygen-containing atmosphere, the electromotive forces of the oxygen concentration cell are measured. Typical result using the sample of $x = 0.03$ as a solid electrolyte is shown in Fig. 3. Dry oxygen at 1.01×10^5 Pa and dry O_2-Ar ($P_{O_2} = 1.01 \times 10^4$ Pa) are supplied to the cathode and anode chambers, respectively. The oxide-ionic transport number ($t_O{}^{2-}$) may be determined by comparing the observed electromotive force value (E_{obs}) of oxygen concentration cell with the corresponding theoretical value (E_{cal}) calculated from the Nernst equation [25,26]. The $t_O{}^{2-}(=E_{obs}/E_{cal})$ is calculated to be 0.71–0.73 at 373–523 K, indicating that the samples are mixed conductors by oxygen ion and electron hole in dry oxygen-containing atmosphere.

The H/D isotope effect on conductivity (σ) is usually used to prove proton conduction in sample in water vapor-containing atmosphere [14,23,27]. The isotope effect may be estimated by the ratio of pre-exponential factors, A_D/A_H. The pre-exponential factor A may be obtained turning to experimental results through the Arrhenius equation:

$$\sigma T = A \exp\left(\frac{-E_a}{k}\right)$$

where E_a is the activation energy and k the Boltzmann constant [28]. Typical result is shown in Fig. 4. It can be seen that the conductivity in H_2O–Ar atmosphere is higher than that in D_2O–Ar atmosphere. The A_D/A_H value for $x = 0.03$ is 1.44, which is close to $1 < A_D/A_H <$

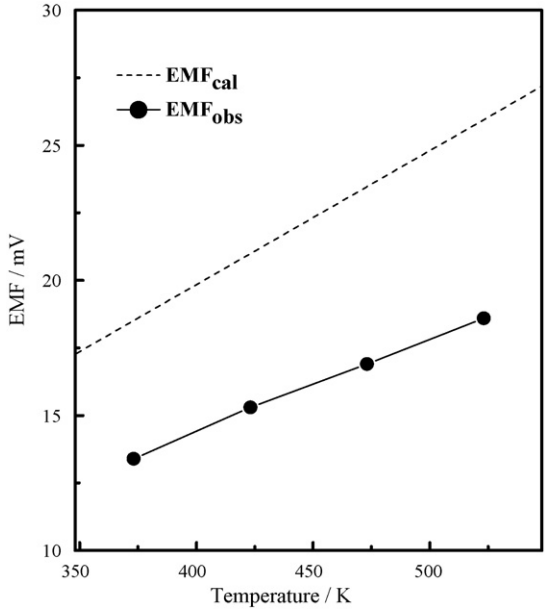

Fig. 3. EMFs of the dry oxygen concentration cell: dry O_2 (1.01×10^5 Pa), Pt|$Sn_{1-x}Ga_xP_2O_7$ ($x = 0.03$)|Pt, dry O_2–Ar ($P_{O_2} = 1.01 \times 10^4$ Pa). The operating temperatures were from 373 K to 523 K. Dotted lines indicate the theoretical values at each temperature.

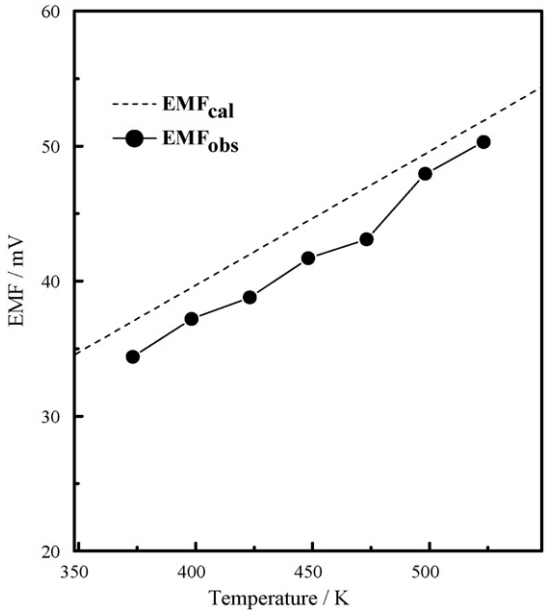

Fig. 5. EMFs of the hydrogen concentration cell: H_2, Pt|$Sn_{1-x}Ga_xP_2O_7$ ($x = 0.03$)|Pt, H_2–Ar ($P_{H_2} = 1.01 \times 10^4$ Pa). The operating temperatures were from 373 K to 523 K. Dotted lines indicate the theoretical values at each temperature.

$\sqrt{2}$ [28], indicating that the sample possesses protonic conduction in water vapor-containing atmosphere.

The ionic transport number (t_i) in wet hydrogen atmosphere may be evaluated by using a similar method as shown in Fig. 3. Fig. 5 shows representative electromotive force results. The ionic transport number $t_i (= E_{obs}/E_{cal})$ is calculated to be 0.92–0.97 at 373–523 K, which is lower than the corresponding theoretical value. It may be ascribed to an electronic conduction in the sample to some extent besides ionic conduction in hydrogen atmosphere. The results in Figs. 4 and 5 suggest that protons are the major charge carriers and it is reasonable to neglect oxygen transport [15,23].

Fig. 6 shows Arrhenius plots of the bulk conductivities of the samples in dry air and wet H_2 atmospheres from 323 K to 523 K. It is clear that the conductivities of the Ga^{3+} doped samples are higher than the conductivities of undoped SnP_2O_7. The highest conductivities were observed for the sample of $x = 0.09$ to be 4.6×10^{-2} S cm^{-1} in wet H_2 and 2.9×10^{-2} S cm^{-1} in dry air at 448 K, respectively, which are about one order of magnitude higher than undoped SnP_2O_7 under the same conditions.

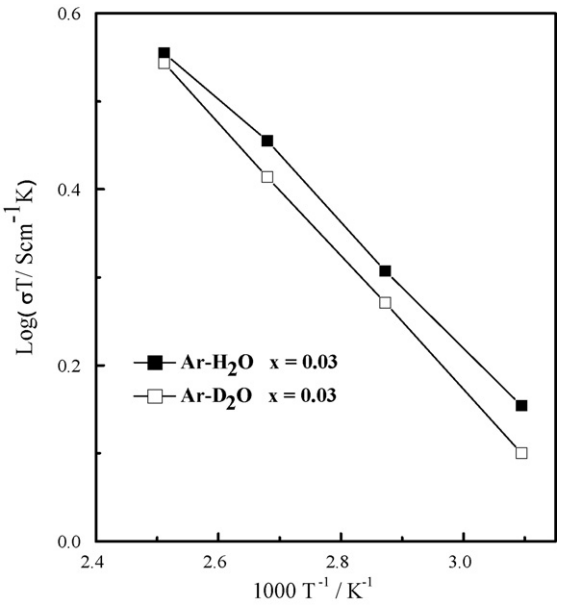

Fig. 4. Isotope effect on conductivity of $Sn_{1-x}Ga_xP_2O_7$ ($x = 0.03$) in argon saturated with H_2O or D_2O vapor at 298 K.

The conduction in the samples may be interpreted in terms of defect chemistry. The higher conductivities of the Ga^{3+} doped samples are resulted from the higher oxygen vacancy concentration. Similar to $BaCeO_3$– and $LaGaO_3$ – based perovskite ceramics [25,29], while partially substituting Sn^{4+} with Ga^{3+} ions, charge compensation is achieved through the formation of oxygen vacancies as indicated by the Eq. (1).

$$2Sn_{Sn}^{\times} + O_O^{\times} + Ga_2O_3 \rightarrow 2Ga_{Sn}' + V_O^{\cdot\cdot} + 2SnO_2 \quad (1)$$

It can be seen that mixed conduction of oxygen ion and electron hole is resulted from Eq. (2) in dry oxygen-containing atmosphere, which is agreed well with the experimental results in Fig. 3.

$$(1/2)O_2 + V_O^{\cdot\cdot} \Leftrightarrow O_o^{\times} + 2h^{\cdot} \quad (2)$$

When water vapor is introduced, as shown in Eq. (3) and (4), the conduction of electron hole and oxygen vacancy decreases, at the same time, the protonic conduction appears. In wet H_2, the protonic conduction may be further improved according to Eq. (3)–(5), resulting in the prevailing protonic conduction in hydrogen atmosphere.

$$H_2O\,(g) + V_O^{\cdot\cdot} + O_o^{\times} \Leftrightarrow 2OH_O^{\bullet} \quad (3)$$

$$H_2O\,(g) + 2h^{\bullet} + 2O_o^{\times} \Leftrightarrow 2OH_O^{\bullet} + (1/2)O_2 \quad (4)$$

$$H_2 + 2O_o^{\times} + 2h^{\bullet} \Leftrightarrow 2OH_O^{\bullet} \quad (5)$$

The influence of the doping level of Ga^{3+} at Sn^{4+} sites on the conductivities may be attributed to the effective concentration of oxygen vacancy in the samples. On one hand, the total concentration of oxygen vacancy $V_O^{\cdot\cdot}$ mainly increases with the increasing of the doping level of Ga^{3+}. On the other hand, the concentrations of point defect pairs, $Ga_{Sn}'V_O^{\cdot\cdot}$, $Ga_{Sn}'V_O^{\cdot\cdot}Ga_{Sn}'$ and $Ga_{Sn}'OH_O^{\bullet}$, which resulted from the coulombic attraction among the point defects with opposite charges, also increase at the same time. Considering the opposite two factors above, the effective concentrations of

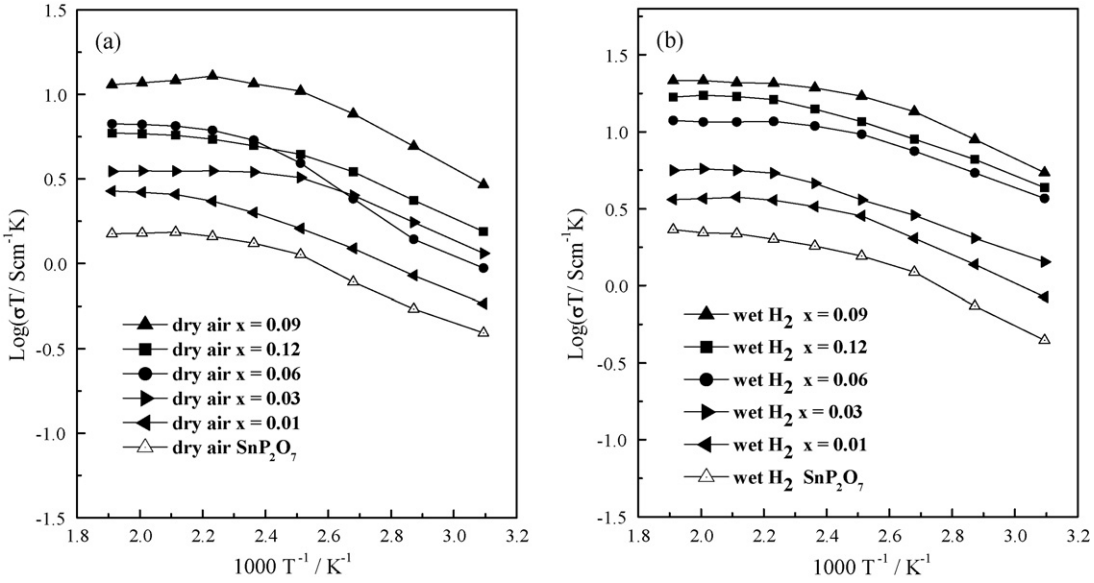

Fig. 6. Temperature dependence of electrical conductivity of SnP_2O_7 and $Sn_{1-x}Ga_xP_2O_7$ ($x = 0.01 - 0.12$) in (a) dry air and (b) wet H_2.

oxygen vacancy may reach its largest value at $x = 0.09$. Moreover, the impurity phase of SnO_2 in the samples for $x > 0.09$ may be also responsible for the decrease in the conductivities. Therefore, these factors result in the highest conductivity at $x = 0.09$.

3.3. Performance of H_2/air fuel cell

Fig. 7 shows the current–voltage–power (I–V–P) curves of the H_2/air fuel cell: wet H_2 ($P_{H_2O} = 3.2 \times 10^3$ Pa), Pt|$Sn_{1-x}Ga_xP_2O_7$ ($x = 0.09$)|Pt, wet Air ($P_{H_2O} = 3.2 \times 10^3$ Pa). The operating temperatures are 423 K and 448 K. On the base of the above discussion, it may be concluded that the samples can exhibit both protonic and oxide-ionic conduction, which is similar to the conclusion reported by Wang et al for $Sn_{0.9}In_{0.1}P_2O_7$ [17]. Therefore, the electrode and cell reactions of the fuel cell may be given as:

$$\text{Anode reaction}: \quad 2H_2 + O^{2-} = 2H^+ + H_2O(A) + 4e^-$$

$$\text{Cathode reaction}: \quad 2H^+ + O_2 + 4e^- = H_2O(C) + O^{2-}$$

$$\text{Cell reaction}: 2H_2 + O_2 = H_2O(A) + H_2O(C)$$

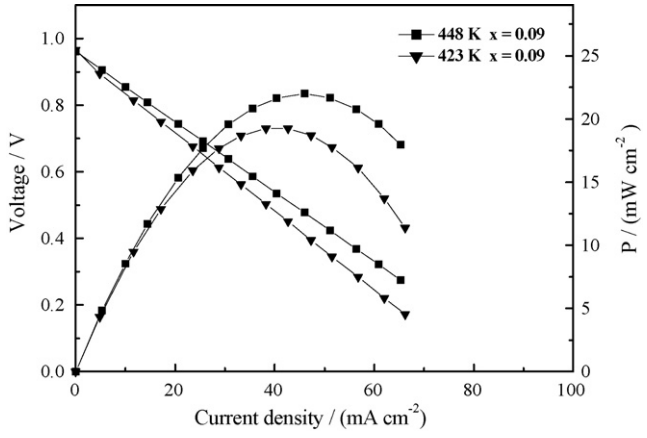

Fig. 7. I–V–P curves for a hydrogen/air fuel cell using $Sn_{1-x}Ga_xP_2O_7$ ($x = 0.09$) as electrolyte at 423 K and 448 K. Electrolyte thickness: 1.45 mm.

The theoretical electromotive force value (EMF) of the fuel cell may be calculated by following Nernst equation [30]:

$$\text{EMF} = \frac{RT}{4F}\left\{\ln K - \ln\left[\frac{P_{H_2O}(A)\cdot P_{H_2O}(C)}{P^2_{H_2}(A)\cdot P_{O_2}(C)}\right]\right\}$$

where K represents the equilibrium constant of the fuel cell reaction at corresponding temperatures, while R, T and F have their usual meanings. P_{O_2} (C), P_{H_2} (A) represent respectively the partial pressures in cathode and anode chambers, P_{H_2O} is controlled by letting gas pass through water at 298 K ($P_{H_2O} = 3.2 \times 10^3$ Pa). As shown in Fig. 7, the open circuit voltages are 0.966 V at 423 K and 0.961 V at 448 K, which are lower than the theoretical values (1.216 V at 423 K and 1.211 V at 448 K). This difference may be relevant to the electronic conduction in the sample as shown in Figs. 3 and 5. It can be seen from Fig. 7 that the peak power densities of this cell reach 19.2 mW cm^{-2} at 423 K and 22.1 mW cm^{-2} at 448 K, correspondingly. The output performance of this cell is not too ideal because we use a thick electrolyte with 1.45 mm. It may be expected that the improvement of fuel cell performance may be achieved through modifying the interface of electrolyte and reducing the thickness of electrolyte.

4. Conclusions

In this study, a novel series of intermediate temperature solid ion conductors, $Sn_{1-x}Ga_xP_2O_7$, is prepared. The doping limit of Ga^{3+} in SnP_2O_7 is 9 mol%. The highest conductivities are observed for the sample of $x = 0.09$ to be 4.6×10^{-2} S cm^{-1} in wet H_2 and 2.9×10^{-2} S cm^{-1} in dry air at 448 K, respectively. The H/D isotope effect on the conductivity confirmed a protonic conduction in the samples in water vapor-containing atmosphere. The mixed conduction of oxygen ion and electron hole in the samples in dry oxygen-containing atmosphere is proved through an oxygen concentration cell method. The peak power densities of H_2/air fuel cell for $x = 0.09$ (thickness: 1.45 mm) reach 19.2 mW cm^{-2} at 423 K and 22.1 mW cm^{-2} at 448 K, respectively. The result indicates that $Sn_{0.91}Ga_{0.09}P_2O_7$ may be used as a potential electrolyte candidate for the intermediate temperature fuel cell.

Acknowledgements

This work was supported by the National Natural Science Foundation of China (No. 20771079) and Anhui province subsidizing Project (Nos. 2007jq1142 and 2008Z038).

References

[1] B.C.H. Steele, A. Heinzel, Nature 414 (2001) 345.
[2] A. Weber, E.I. Tiffee, J. Power Sources 127 (2004) 273.
[3] T. Norby, Nature 410 (2001) 877.
[4] G. Adachi, N. Imanaka, S. Tamura, Chem. Rev. 102 (2002) 2405.
[5] S.M. Haile, D.A. Boysen, C.R.I. Chisholm, R.B. Merle, Nature 410 (2001) 910.
[6] E.P. Murray, T. Tsai, S.A. Barnett, Nature 400 (1999) 649.
[7] K. Xie, R.Q. Yan, X.X. Xu, X.Q. Liu, G.Y. Meng, J. Power Sources 187 (2009) 403.
[8] H. Zhong, H. Matsumoto, T. Ishihara, A. Toriyama, J. Power Sources 186 (2009) 238.
[9] A.M. Amesti, A. Larranaga, L.M.R. Martínez, M.L. Nó, J.L. Pizarro, A. Laresgoiti, M.I. Arriortua, J. Power Sources 192 (2009) 151.
[10] H.D. Lin, C.J. Zhao, H. Na, J. Power Sources 195 (2010) 3380.
[11] H.L. Wang, J.A. Turner, J. Power Sources 183 (2008) 576.
[12] J.J. Li, F. Ye, L. Chen, T.T. Wang, J.L. Li, X.D. Wang, J. Power Sources 186 (2009) 320.
[13] D.A. Boysen, T. Uda, C.R.I. Chisholm, S.M. Haile, Science 303 (2004) 68.
[14] M. Nagao, T. Kamiya, P. Heo, A. Tomita, T. Hibino, M. Sano, J. Electrochem. Soc. 153 (2006) A1604.
[15] A. Tomita, N. Kajiyama, T. Kamiya, M. Nagao, T. Hibino, J. Electrochem. Soc. 154 (2007) B1265.
[16] S.W. Tao, Solid State Ions 180 (2009) 148.
[17] X. Chen, C.S. Wang, E.A. Payzant, C.R. Xia, D. Chu, J. Electrochem. Soc. 155 (2008) B1264.
[18] X. Wu, A. Verma, K. Scott, Fuel Cells 8 (2008) 453.
[19] K. Genzaki, P. Heo, M. Sano, T. Hibino, J. Electrochem. Soc. 156 (2009) B806.
[20] A. Tomita, T. Yoshii, S. Teranishi, M. Nagao, T. Hibino, J. Catal. 247 (2007) 137.
[21] A. Tomita, J. Nakajima, T. Hibino, Angew. Chem. Int. Ed. 47 (2008) 1462.
[22] S. Teranishi, K. Kondo, A. Tsuge, T. Hibino, Sens. Actuators B 140 (2009) 170.
[23] M. Nagao, A. Takeuchi, P. Heo, T. Hibino, M. Sano, A. Tomita, Electrochem. Solid-State Lett. 9 (2006) A105.
[24] R.D. Shannon, Acta Cryst. A32 (1976) 751.
[25] G.L. Ma, F. Zhang, J.L. Zhu, G.Y. Meng, Chem. Mater. 18 (2006) 6006.
[26] F. Zhang, Q. Yang, B. Pan, R. Xu, H.T. Wang, G.L. Ma, Mater. Lett. 61 (2007) 4144.
[27] T. Norby, Solid State Ionics 40–41 (1990) 857.
[28] A.S. Nowick, A.V. Vaysleyb, Solid State Ionics 97 (1997) 17.
[29] Y.X. Guo, B.X. Liu, C. Chen, W.B. Wang, G.L. Ma, Electrochem. Commun. 11 (2009) 153.
[30] G.L. Ma, L.G. Qiu, R. Chen, Acta Chim. Sinica 60 (2002) 2135 (in Chinese).